Comparison Study of Strong-Field Ionization of Molecules and Atoms by Bicircular Two-Color Femtosecond Laser Pulses

Kang Lin,[1] Xinyan Jia,[2] Zuqing Yu,[3] Feng He,[3] Junyang Ma,[1] Hui Li,[1] Xiaochun Gong,[1] Qiying Song,[1] Qinying Ji,[1] Wenbin Zhang,[1] Hanxiao Li,[1] Peifen Lu,[1] Heping Zeng,[1] Jing Chen,[4,5,*] and Jian Wu[1,6,†]

[1]*State Key Laboratory of Precision Spectroscopy, East China Normal University, Shanghai 200062, China*
[2]*School of Physical Science and Technology, Southwest Jiaotong University, Chengdu 610031, China*
[3]*Key Laboratory of Laser Plasmas (Ministry of Education) and School of Physics and Astronomy, Collaborative Innovation Center for IFSA (CICIFSA), Shanghai Jiao Tong University, Shanghai 200240, China*
[4]*HEDPS, Center for Applied Physics and Technology, Peking University, Beijing 100084, China*
[5]*Institute of Applied Physics and Computational Mathematics, P.O. Box 8009, Beijing 100088, China*
[6]*Collaborative Innovation Center of Extreme Optics, Shanxi University, Taiyuan, Shanxi 030006, China*

(Received 22 May 2017; revised manuscript received 21 September 2017; published 15 November 2017)

We experimentally investigate the single and double ionization of N_2 and O_2 molecules in bicircular two-color femtosecond laser pulses, and compare with their companion atoms of Ar and Xe with comparable ionization thresholds. Electron recollision assisted enhanced ionization is observed in N_2 and Ar by controlling the helicity and field ratio between the two colors, whereas the enhanced ionization via the recollision is almost absent in O_2 and Xe. Our *S*-matrix simulations clearly reveal the crucial role of the detailed electronic structures of N_2 and O_2 on the two-dimensional recollision of the electrons driven by the bicircular two-color laser fields. As compared to Ar, the resonant multiphoton excitation dominates the double ionization of Xe.

DOI: 10.1103/PhysRevLett.119.203202

Bound electrons in atoms and molecules can be released to continua when exposed to strong laser fields, in which scenario freed electrons may be driven back to recombine with parent ions leading to the emission of high harmonics or attosecond bursts in extremely ultraviolet spectrum [1–3], or to kick out a second electron resulting in the nonsequential double ionization (NSDI) [4,5]. The field-driven rescattering [6] of freed electrons can be used to image molecular structure, termed as the laser-induced electron diffraction [7,8], with attosecond temporal and subangstrom spatial resolution. In general, these electron-nuclei recollision processes are favored for linearly polarized laser fields as compared to circular polarization which drives the liberated electrons away from the parent nuclear cores [9–11].

Interestingly, the high-harmonic generation [12,13] and electron-ion rescattering [14–18] of atoms were recently demonstrated using counterrotating circularly polarized two-color laser fields [19,20], as illustrated in the inset of Fig. 1. Depending on the helicity and relative strength between the two colors, the motion of the liberated electron and thus the recollision process can be spatiotemporally manipulated [16–18]. The NSDI dynamics of He and Ar driven by the counterrotating two-color laser fields are very similar, with an optimal intensity ratio between the two colors for maximizing the probability of electron recollision [16–18]. However, so far this study is mostly limited to low-Z atoms, e.g., He and Ar [16–18]. For molecules, where more degrees of freedom and complicated electronic structures are involved [21,22], the study of the bicircular two-color laser field assisted electron recollision is lacking yet. For instance, it was demonstrated that N_2 exhibits atomlike behaviors in single and double ionization induced by linearly and circularly polarized laser fields [23,24], while O_2 exhibits noticeable ionization suppression in comparison with Xe [25–29].

In this Letter, we report on the comparison study of the strong-field ionization of N_2 and O_2 molecules driven by bicircular two-color laser fields, along with their companion atoms of Ar and Xe. We find the optimization strategy for maximizing the electron recollision probability

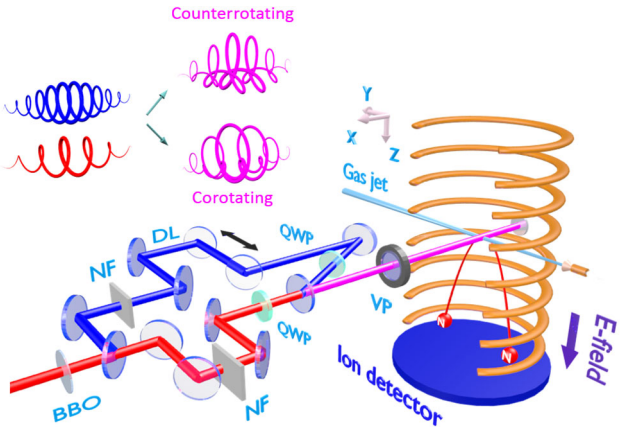

FIG. 1. Experimental setup. DL: delay line; QWP: quarter wave plate; VP: view port; NF: neutral filter. Inset: time-dependent electric field of the counterrotating and corotating two-color fields.

is not only determined by the helicity and intensity ratio between the two colors but also strongly depends on the species of the target, which can be traced back to the detailed electronic structure. The electron recollision enhanced ionization is significant in N_2 and Ar, while this recollision process is hard to be observed in O_2 and Xe. The *S*-matrix simulations clearly reveal the crucial role of the electronic structures of N_2 and O_2 molecules on the recollision-assisted enhanced ionziation. Our results show the discrepancy in controlling the electron recollision dynamics between molecules and atoms using circularly polarized two-color laser fields, which is implicative for further important applications [12,13] and steering two-dimensional electron motion in molecules [30].

As schematically illustrated in Fig. 1, we create the bicircular two-color fields by frequency doubling a linearly polarized femtosecond laser pulse (25 fs, 790 nm, 10 kHz), followed by further circular polarization shaping to have the same or opposite helicities. The counterrotating or corotating two-color fields are then collimated to focus onto the supersonic gas jet of the mixture of N_2 and Ar (1:1) or O_2 and Xe (9:1) in the apparatus of COLTRIMS (cold target recoil ion momentum spectroscopy) [31]. The relative intensity between the two colors is adjusted via two neutral filters in the fundamental-wave (FW) and second-harmonic (SH) paths. See the Supplemental Material [32] for more details of experiments.

Figures 2(a) and 2(b) show the measured yields of various fragment ions produced from the N_2 and Ar

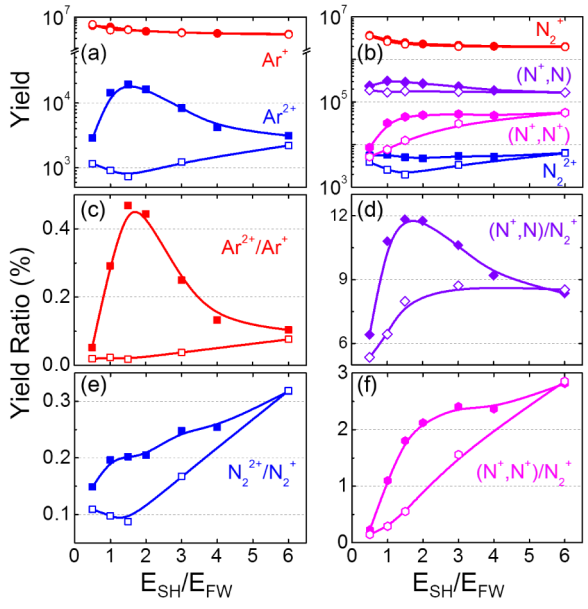

FIG. 2. Single and double ionization yields of Ar and N_2 driven by bicircular two-color laser fields. Solid and hollow symbols represent the counter- and co-rotating cases, respectively. (a) and (b) are the measured ion yields, and (c)-(f) are the yield ratios of different channels. The solid curves are numerical fits of the experimental data.

mixture irradiated by the bicircular two-color laser fields as a function of the relative strength of the electric fields between the two colors, i.e., E_{SH}/E_{FW}. The combined intensity of the two-color laser fields is kept constant $\sim 5.0 \times 10^{14}$ W/cm^2 for various field ratios, which is confirmed by the nearly flat single ionization yields of N_2^+ and Ar^+ as shown in Figs. 2(a) and 2(b). Each data point is normalized to 2.5 million laser shots. The detection efficiency of microchannel plate (MCP) for different ion species is taken into account [23,33]. The yields of Ar^+ [Fig. 2(a)] and N_2^+ [Fig. 2(b)] are similar because of their comparable single ionization thresholds (N_2: 15.58 eV; Ar: 15.76 eV) [23]. Interestingly, although they have similar double ionization thresholds (N_2: 27.12 eV; Ar: 27.63 eV) [23], their doubly charged ion yields exhibit anomalous diversity versus the field ratio. As shown in Fig. 2(a), the Ar^{2+} yield in a counterrotating case rises rapidly with the increasing of the relative strength of the *SH* field, peaking around $E_{SH}/E_{FW} = 1.5$, followed by falling down gradually, agreeing with previous observations [18]. The significant enhancement of the Ar^{2+} yield in the counterrotating fields clearly indicates the contribution of electron recollision on the double ionization of Ar which is absent in the corotating fields [16–18]. The freed electrons in the counterrotating fields experience two-dimensional close-loop trajectories, leading to much higher probability to encounter the parent ions and knock out a second electron or to excite the parent ions followed by subsequent field ionization. To quantify the ionization enhancement from the electron recollision, we plot the yield ratio between the counterrotating and corotating cases in Fig. 3(a). An enhancement factor of 26 is observed around $E_{SH}/E_{FW} = 1.5$, clearly elucidating significant manipulation of the electron recollision assisted NSDI by controlling the field ratio of the counterrotating two-color laser fields.

For molecules, the situation becomes more intriguing since various ionization channels may open via different mechanisms. The results of N_2 molecule are shown in Fig. 2(b). At first glance, except N_2^+, the yields of dication N_2^{2+}, dissociative single and double ionization channels, $N_2 + n_1\hbar\omega \rightarrow N^+ + N + e$, $N_2 + n_2\hbar\omega \rightarrow N^+ + N^+ + 2e$, denoted as ($N^+$, N) and ($N^+$, N^+), respectively, all display obvious enhancement in the counterrotating fields as compared to the corotating one. To increase the visibility, we plot the relative yields of individual channels with respect to the N_2^+ in Figs. 2(d), 2(e), and 2(f) separately. The relative yield of $(N^+, N)/N_2^+$ in the counterrotating case exhibits similar field-ratio dependence as Ar^{2+}/Ar^+, which peaks around $E_{SH}/E_{FW} = 1.5$. While for the corotating case the relative yield of $(N^+, N)/N_2^+$ increases greatly with the field ratio and finally saturates after $E_{SH}/E_{FW} = 3$. It is caused by the photon-coupling assisted dissociation of N_2^+ which is favored with the increasing of the *SH* field. However, the enhanced yield of the (N^+, N) in the counterrotating two-color laser

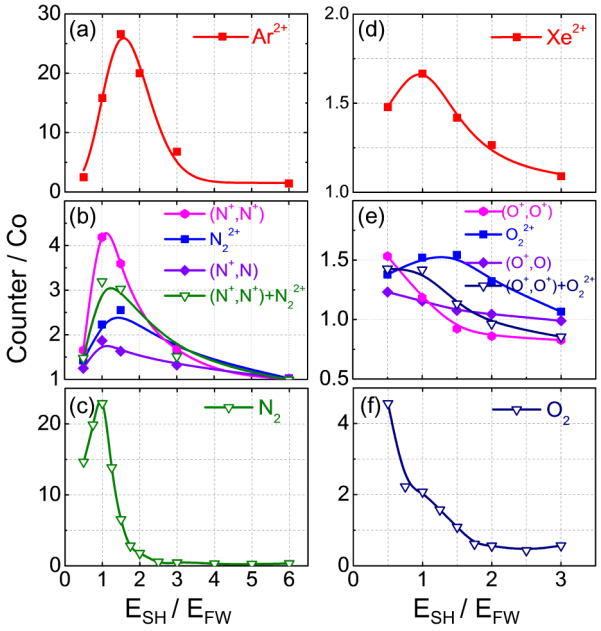

FIG. 3. Experimentally measured yield ratios between counterrotating and corotating cases of (a) Ar, (b) N_2, (d) Xe, and (e) O_2, respectively. The numerically simulated yield ratios of N_2 and O_2 molecules are correspondingly plotted in (c) and (f). The solid curves are numerical fits of the measured and simulated data.

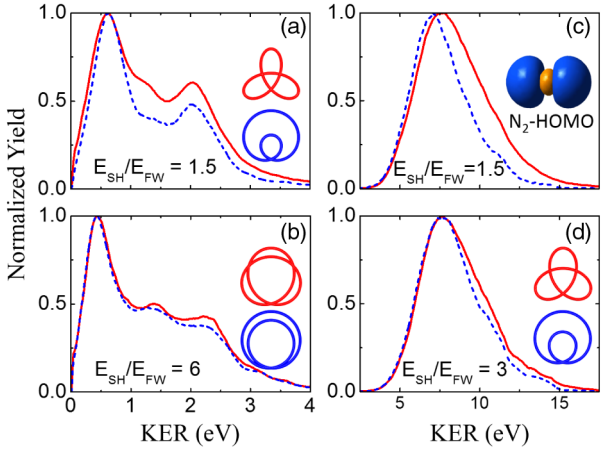

FIG. 4. KER spectra of (a), (b) (N^+, N) and (c),(d) (N^+, N^+) channels at different field ratios of E_{SH}/E_{FW} between the counterrotating (red solid curves) and corotating (blue dashed curves) bicircular two-color laser fields. The insets in (a), (b), and (d) are the electric fields of the counterrotating and corotating cases at corresponding field ratios. The inset of (c) is the shape of the HOMO of N_2.

fields is contributed by the electron recollision induced excitation of the N_2^+, which subsequently dissociates into the (N^+, N) channel. It is confirmed by examining the kinetic energy release (KER) of the ejected nuclear fragments, as shown in Figs. 4(a) and 4(b). Noticeable enhanced yield at high KER of the (N^+, N) channel in the counterrotating two-color laser fields with respect to that of the corotating case is observed for $E_{SH}/E_{FW} = 1.5$, which dramatically reduces for $E_{SH}/E_{FW} = 6.0$ when the (N^+, N) yields are the same for the counter and corotating cases. The increment of high-KER nuclear fragments clearly reveals the important role of the electron recollision in generating the (N^+, N) channel in the counterrotating two-color laser fields.

Interestingly, different field-ratio dependences are observed in the double ionization channels of N_2^{2+} and (N^+, N^+), as shown in Figs. 2(e) and 2(f). As compared to the corotating fields, the relative yields of N_2^{2+}/N_2^+ and $(N^+, N^+)/N_2^+$ in the counterrotating fields exhibit similar knee structures as a function of the field ratio resulting from the field-driven recollision of the liberated electrons, in analogy to the typical characteristic manifesting the NSDI in atoms at moderate laser intensities [4,5]. The electron recollision mainly contributes to the generation of high-KER nuclear fragments of the (N^+, N^+) channel as displayed in Figs. 4(c) and 4(d), which becomes negligible when the field ratio increases from $E_{SH}/E_{FW} = 1.5$ to 3. The electron recollision contribution is more significant (~2 times) in producing the (N^+, N^+) channel as compared to the N_2^{2+}, as shown in Fig. 3(b). We note that the yields of all three channels of (N^+, N), N_2^{2+}, and (N^+, N^+) show Ar-like peaking structures where the field ratio of the counterrotating two-color laser field is optimal to maximize the electron recollision probability.

In the following by using the bicircular two-color laser fields, we focus on the comparison between O_2 and Xe where more elaborate strong-field ionization dynamics are observed. Since the ionization potentials of O_2 and Xe (O_2: 12.06 eV; Xe: 12.13 eV) [23] are lower than N_2 and Ar, the combined intensity of the two-color fields is reduced to $\sim 3.5 \times 10^{14}$ W/cm^2. Figures 5(a) and 5(b) show the experimental results of Xe and O_2, respectively. Differing from Ar, no peaking structure is observed in the yield of Xe^{2+} versus the field ratio between the two colors in counterrotating or corotating cases. More clearly, as shown in Fig. 5(c), the relative yields of Xe^{2+}/Xe^+ in both helicities show the same tendency of monotonic increment. The similarity among the two helicities in field-ratio dependence implies the negligible contribution from the electron recollision process. As compared to Ar, the multiphoton resonant process via the intermediate states dominates the double ionization of Xe [34,35]. For fixed intensity of the combined field in our experiments, as the increasing of the relative strength of the *SH* field, the role of the multiphoton double ionization is enhanced gradually and thus the yield of the Xe^{2+} regardless of the helicities of the two colors. As shown in Fig. 3(d), the minor enhancement of the Xe^{2+} yield in the counterrotating two-color laser fields as compared to the corotating one, ~15 times smaller than Ar, confirms the negligible contribution from the electron recollision as compared to the multiphoton resonance in double ionization of Xe.

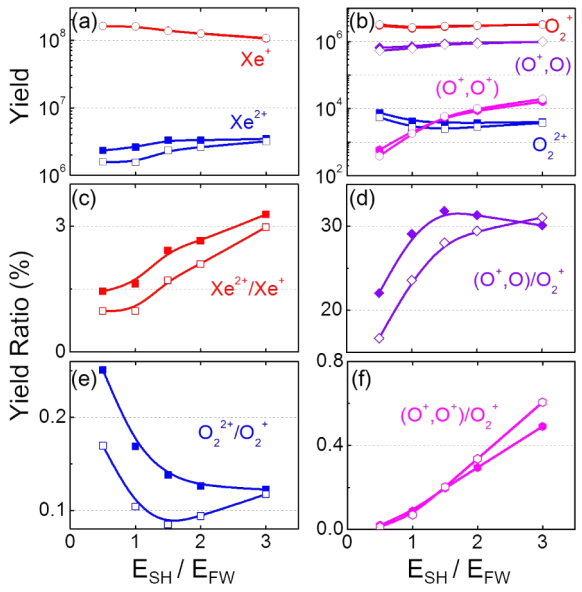

FIG. 5. Same as Fig. 2 but for various ionization channels of Xe and O_2. The solid curves are numerical fits of the experimental data.

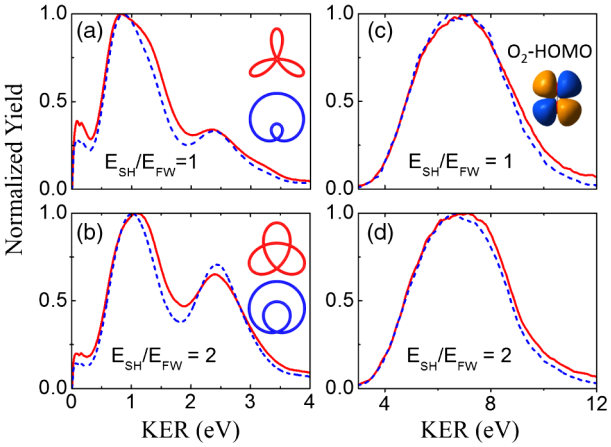

FIG. 6. Same as Fig. 4 but for(a),(b) (O^+, O) and (c), (d) (O^+, O^+) channels of O_2.

Although the ionization threshold of O_2 is comparable to Xe, the production of O_2^+ suffers conspicuous ionization suppression as compared to Xe^+ in both counterrotating and corotating two-color laser fields, as shown in Fig. 5(b). The single ionization suppression of the O_2 molecule in a single-color laser field has been studied for decades [25–28]. Here we provide the first experimental observation of this suppression phenomenon in bicircular two-color fields. Figures 5(d)–5(f) display the relative yields of $(O^+, O)/O_2^+$, O_2^{2+}/O_2^+, $(O^+, O^+)/O_2^+$ versus the field ratio between the two colors, respectively. In contrast to N_2, only a very small enhancement is observed for the single and double ionization of O_2 in the counterrotating two-color laser fields as compared to the corotating one. The overall increment of the recollision-enhanced ionization of O_2 between the counterrotating and corotating cases is much smaller than N_2 [Fig. 3(e)]. As shown in Fig. 6, the KER spectra of the (O^+, O) and (O^+, O^+) channels are almost the same for the counterrotating and corotating fields and weakly depend on the field ratio, indicating the inactivation of the electron recollision dynamics here.

Despite the different hypotheses that are proposed for understanding the underlying physics of single [25–27] and double [36–39] ionization suppression of the O_2 molecule, the consensus is mostly based on the antisymmetric electronic structure of the outermost orbital of O_2. The influence of the detailed electronic structure of molecules on the rescattering dynamics in linearly polarized laser field reveals that different mechanisms account for the double ionization of N_2 and O_2 [37]. Here, as shown in Figs. 3(c) and 3(f), the experimentally observed difference between N_2 and O_2 versus the field ratio between the two colors of bicircular laser fields can be qualitatively reproduced by the S-matrix simulations [38,39]. The ratio between the counterrotating and corotating fields peaks around $E_{SH}/E_{FW} = 1$ for N_2 [Fig. 3(c)]. In contrast, the ratio of O_2 monotonically decreases with the field ratio E_{SH}/E_{FW} [Fig. 3(f)]. It should be noted that the individual channel [X_2^{2+} and (X^+, X^+)] cannot be distinguished in our current model; therefore the calculated result should be compared with the sums of X_2^{2+} and (X^+, X^+) channels in experiment, which are also depicted in Figs. 3(b) and 3(e) and show good agreements with the simulation: the ratio of N_2 peaks at $E_{SH}/E_{FW} = 1$ and the ratio of O_2 decreases monotonically. The difference between the two molecules can be attributed to strong suppression of the electron recollision-assisted NSDI of O_2 with respect to that of N_2. It can be explained by different angular distributions of the first freed photoelectron of N_2 and O_2 considering that N_2 has a $3\sigma_g$ outmost orbital while the outmost orbital of O_2 is $1\pi_g$ [38,39]. See the Supplemental Material [32] for more details of numerical simulations.

Furthermore, the O_2^{2+} and (O^+, O^+) channels exhibit opposite dependence on the field ratio in both helicities. For simplicity, we consider the case of corotating two-color laser fields where the electron recollision enhancement is eliminated. The yield of O_2^{2+} and (O^+, O^+) decreases and increases, respectively, as the ratio of the field strength E_{SH}/E_{FW} increases. The diversity indicates different mechanisms in producing O_2^{2+} and (O^+, O^+) by releasing electrons from different orbitals [24]. The (O^+, O^+) is dominated by the sequential process accompanied with the electron removal from the lower-lying orbitals, which differs from the O_2^{2+} where a certain amount of NSDI is involved by releasing two electrons from the highest occupied molecular orbital [24].

In conclusion, the comparison study of the strong-field ionization of molecules and atoms using counterrotating and corotating two-color laser fields enables us to

unambiguously discriminate the field-driven electron recollision dynamics. Depending on the relative helicity and field strength between the two colors, the recollision of the liberated electrons can be significantly enhanced for the strong-field ionization of N_2 and Ar. The recollision dynamics in strong-field ionization of O_2 is dramatically suppressed owing to the antisymmetric profile of the outermost orbital. Since the double ionization of Xe is dominated by the resonant multiphoton process, the electron recollision plays a minor role in the double ionization of Xe. Our results are more likely to inspire further applications of the bicircular two-color fields in wide areas, e.g., direct circular high harmonics and attosecond bursts generation [13], THz radiation [40], and ultrashort spinning electron pulse creation [41].

This work is supported by the National Key program for S&T Research and Development of China (No. 2016YFA0401100), the National Basic Research Program of China (No. 2013CB922201), the National Natural Science Fund of China (Grants No. 11425416, No. 61690224, No. 11621404, No. 11322438, No. 11574205, No. 11334009, and No. 11425414), and the 111 project of China (Grant No. B12024).

*chen_jing@iapcm.ac.cn
†jwu@phy.ecnu.edu.cn

[1] A. Mcpherson, G. Gibson, H. Jara, U. Johann, T. S. Luk, I. A. McIntyre, K. Boyer, and C. K. Rhodes, J. Opt. Soc. Am. B **4**, 595 (1987).
[2] J. L. Krause, K. J. Schafer, and K. C. Kulander, Phys. Rev. Lett. **68**, 3535 (1992).
[3] D. Popmintchev *et al.*, Science **350**, 1225 (2015).
[4] D. N. Fittinghoff, P. R. Bolton, B. Chang, and K. C. Kulander, Phys. Rev. Lett. **69**, 2642 (1992).
[5] B. Walker, B. Sheehy, L. F. DiMauro, P. Agostini, K. J. Schafer, and K. C. Kulander, Phys. Rev. Lett. **73**, 1227 (1994).
[6] P. B. Corkum, Phys. Rev. Lett. **71**, 1994 (1993).
[7] C. I. Blaga, J. Xu, A. D. DiChiara, E. Sistrunk, K. Zhang, P. Agostini, T. A. Miller, L. F. DiMauro, and C. D. Lin, Nature (London) **483**, 194 (2012).
[8] M. G. Pullen, B. Wolter, A.-T. Le, M. Baudisch, M. Hemmer, A. Senftleben, C. D. Schröter, J. Ullrich, R. Moshammer, C. D. Lin, and J. Biegert, Nat. Commun. **6**, 7262 (2015).
[9] P. Dietrich, N. H. Burnett, M. Ivanov, and P. B. Corkum, Phys. Rev. A **50**, R3585 (1994).
[10] W. Becker, F. Grasbon, R. Kopold, D. B. Milošević, G. G. Paulus, and H. Walther, Adv. At. Mol. Opt. Phys. **48**, 35 (2002).
[11] W. A. Bryan, S. L. Stebbings, J. McKenna, E. M. L. English, M. Suresh, J. Wood, B. Srigengan, I. C. E. Turcu, J. M. Smith, E. J. Divall, C. J. Hooker, A. J. Langley, J. L. Collier, I. D. Williams, and W. R. Newell, Nat. Phys. **2**, 379 (2006).
[12] A. Fleischer, O. Kfir, T. Diskin, P. Sidorenko, and O. Cohen, Nat. Photonics **8**, 543 (2014).
[13] O. Kfir, P. Grychtol, E. Turgut, R. Knut, D. Zusin, D. Popmintchev, T. Popmintchev, H. Nembach, J. M. Shaw, A. Fleischer, H. Kapteyn, M. Murnane, and O. Cohen, Nat. Photonics **9**, 99 (2015).
[14] C. A. Mancuso, D. D. Hickstein, P. Grychtol, R. Knut, O. Kfir, X.-M. Tong, F. Dollar, D. Zusin, M. Gopalakrishnan, C. Gentry, E. Turgut, J. L. Ellis, M.-C. Chen, A. Fleischer, O. Cohen, H. C. Kapteyn, and M. M. Murnane, Phys. Rev. A **91**, 031402 (2015).
[15] C. A. Mancuso, D. D. Hickstein, K. M. Dorney, J. L. Ellis, E. Hasović, R. Knut, P. Grychtol, C. Gentry, M. Gopalakrishnan, D. Zusin, F. J. Dollar, X.-M. Tong, D. B. Milošević, W. Becker, H. C. Kapteyn, and M. M. Murnane, Phys. Rev. A **93**, 053406 (2016).
[16] J. L. Chaloupka and D. D. Hickstein, Phys. Rev. Lett. **116**, 143005 (2016).
[17] C. A. Mancuso, K. M. Dorney, D. D. Hickstein, J. L. Chaloupka, J. L. Ellis, F. J. Dollar, R. Knut, P. Grychtol, D. Zusin, C. Gentry, M. Gopalakrishnan, H. C. Kapteyn, and M. M. Murnane, Phys. Rev. Lett. **117**, 133201 (2016).
[18] S. Eckart, M. Richter, M. Kunitski, A. Hartung, J. Rist, K. Henrichs, N. Schlott, H. Kang, T. Bauer, H. Sann, L. Ph. H. Schmidt, M. Schöffler, T. Jahnke, and R. Dörner, Phys. Rev. Lett. **117**, 133202 (2016).
[19] T. Zuo and A. D. Bandrauk, J. Nonlinear Opt. Phys. Mater. **04**, 533 (1995); A. D. Bandrauk and H. Z. Lu, Phys. Rev. A **68**, 043408 (2003); K. J. Yuan and A. D. Bandrauk, Phys. Rev. A **92**, 063401 (2015).
[20] W. Becker, B. N. Chichkov, and B. Wellegehausen, Phys. Rev. A **60**, 1721 (1999).
[21] S. Odžak, E. Hasović, and D. B. Milošević, Phys. Rev. A **94**, 033419 (2016).
[22] M. Busuladžić, A. Gazibegović-Busuladžić, and D. B. Milošević, Phys. Rev. A **95**, 033411 (2017).
[23] C. Guo, M. Li, J. P. Nibarger, and G. N. Gibson, Phys. Rev. A **58**, R4271 (1998).
[24] C. Guo, M. Li, J. P. Nibarger, and G. N. Gibson, Phys. Rev. A **61**, 033413 (2000).
[25] C. Guo, Phys. Rev. Lett. **85**, 2276 (2000).
[26] J. Muth-Böhm, A. Becker, and F. H. M. Faisal, Phys. Rev. Lett. **85**, 2280 (2000).
[27] X. M. Tong, Z. X. Zhao, and C. D. Lin, Phys. Rev. A **66**, 033402 (2002).
[28] Z. Y. Lin, X. Y. Jia, C. L. Wang, Z. L. Hu, H. P. Kang, W. Quan, X. Y. Lai, X. J. Liu, J. Chen, B. Zeng, W. Chu, J. P. Yao, Y. Cheng, and Z. Z. Xu, Phys. Rev. Lett. **108**, 223001 (2012).
[29] J. Wu, H. Zeng, and C. Guo, Phys. Rev. Lett. **96**, 243002 (2006).
[30] K. Lin, X. Gong, Q. Song, Q. Ji, W. Zhang, J. Ma, P. Lu, H. Pan, J. Ding, H. Zeng, and J. Wu, J. Phys. B **49**, 025603 (2016).
[31] J. Ullrich, R. Moshammer, A. Dorn, R. Dörner, L. Ph. H. Schmidt, and H. Schmidt-Böcking, Rep. Prog. Phys. **66**, 1463 (2003).
[32] See Supplemental Material at http://link.aps.org/supplemental/10.1103/PhysRevLett.119.203202 for details of the numerical simulations.
[33] C. Cornaggia, J. Lavancier, D. Normand, J. Morellec, P. Agostini, J. P. Chambaret, and A. Antonetti, Phys. Rev. A **44**, 4499 (1991).

[34] J. L. Chaloupka, J. Rudati, R. Lafon, P. Agostini, K. C. Kulander, and L. F. DiMauro, Phys. Rev. Lett. **90**, 033002 (2003).
[35] J. Rudati, J. L. Chaloupka, P. Agostini, K. C. Kulander, and L. F. DiMauro, Phys. Rev. Lett. **92**, 203001 (2004).
[36] C. Guo, R. T. Jones, and G. N. Gibson, Phys. Rev. A **62**, 015402 (2000).
[37] E. Eremina, X. Liu, H. Rottke, W. Sandner, M. G. Schätzel, A. Dreischuh, G. G. Paulus, H. Walther, R. Moshammer, and J. Ullrich, Phys. Rev. Lett. **92**, 173001 (2004).
[38] X. Y. Jia, W. D. Li, J. Fan, J. Liu, and J. Chen, Phys. Rev. A **77**, 063407 (2008).
[39] X. Y. Jia, D. H. Fan, W. D. Li, and J. Chen, Chin. Phys. B **22**, 013303 (2013).
[40] C. Meng, W. Chen, X. Wang, Z. Lv Y. Huang, J. Liu, D. Zhang, Z. Zhao, and J. Yuan, Appl. Phys. Lett. **109**, 131105 (2016).
[41] D. B. Milošević, Phys. Rev. A **93**, 051402 (2016).